COMPDYN 2013
4th ECCOMAS Thematic Conference on
Computational Methods in Structural Dynamics and Earthquake Engineering
M. Papadrakakis, N. D. Lagaros, V. Plevris (eds.)
Kos Island, Greece, 12–14 June 2013

ROCKING AND SLIDING OF UNANCHORED BODIES SUBJECTED TO SEISMIC LOAD ACCORDING TO CONVENTIONAL AND NUCLEAR RULES

H. Schau[1] and M. Johannes[2*]

TÜV SÜD Energietechnik GmbH Baden-Württemberg
Dudenstraße 28, 68167 Mannheim, Germany

[1]Henry.Schau@tuev-sued.de
[2]Michael.Johannes@tuev-sued.de

Keywords: Dynamics, Rigid Body, Rocking, Overturning, Seismic Loads, Rules, Impact.

Abstract. *In nuclear and nonnuclear facilities unanchored components like storage casks for spent fuel may cause unacceptable damage in case of an earthquake. It must be proven that the unanchored body will not tip over and/or slide impermissible distances. Rocking and sliding are highly nonlinear phenomena which cannot be completely described analytically. Therefore, the rocking and sliding motion of a rigid body under various conditions will be analysed analytically and numerically by numerical integration of the equations of motion and by using the Finite Element Method (implicit time integration). It is shown that a finite element program with an implicit time integration method can solve the impact problem. By using the Finite Element Method it is possible to investigate the influence of the properties of the base, the contact conditions and slightly deviations from the ideal geometry on the motion of the body and especially on the coefficient of restitution. Additionally, the influence of occasionally used anti-slip pads below the rocking body is investigated. In practice most unanchored bodies are not slender and therefore this paper studies a compact body with an aspect ratio of 2. One focal topic is the discussion of the coefficient of restitution. It is shown that more realistic finite element models, which take into account the above mentioned influences, lead to higher coefficients than those derived analytically from simplified models. The agreement between results from finite element analyses and the numerical integration of the equations of motion is very good if the coefficients of restitution are based on best estimate values from finite element analyses. The dynamic investigations consider an excitation by sine, triangle or rectangle vibrations and time histories from earthquake ground accelerations. It is remarkable, that in the some cases of the amplitudes will increase significantly over time until overturning. The criteria and methods given in European (German) and US standards with regard to overturning and impermissible sliding are presented. The safety margins against overturning and impermissible sliding will be discussed.*

1 INTRODUCTION

In nuclear power plants but also chemical plants unanchored components can cause unacceptable damage in the case of an earthquake (but also of a blast wave or a plane crash). This applies also if the components such as e.g. storage casks are designed for the loads from overturning or hitting. To avoid damage it must be demonstrated that under these loads no overturning or impermissible slipping of unanchored components occurs. Therefore, in this paper the behaviour of unanchored components excited by earthquakes will be analysed. In principle it is the dynamic of a rigid, elastic or plastic body on a rigid, elastic or plastic foundation. The mechanical problem for a rigid body looks simple at the first sight, but becomes difficult due to the impacts. In literature the question of rocking or tilting oscillations of a rigid body has been found to be of great interest, so that there are a large number of publications on the subject. In this context the fundamental works [1] to [7] and further studies [8] to [22] should be mentioned. Based on these works, the dynamics of unanchored bodies, especially for the rocking and sliding of a rigid body under various conditions, will be analysed analytically and numerically by numerical integration of the equations of motion and using the Finite Element Method. Especially the influence of the supporting flexibilities, the material properties of the base, the contact conditions, slight deviations from the ideal geometry and the kind of excitation on the motion of the body will be investigated. In contrast to most other studies more compact bodies are considered. The suitability of an implicit Finite Element Method for such studies will be investigated. Additionally, it is shown, how rocking and sliding are treated in the nuclear and non-nuclear rules.

2 THEORY OF ROCKING AND SLIDING MOTION

A rigid body (block) in a plane subjected to an earthquake excitation can perform the following kinds of motions: Rest, rotation (rocking), sliding, sliding rotation, translation and rotation jump [2]. A plane model to describe the rotation or rocking motion of a rigid body (on a rigid base) is shown in Figure 1, where CG denotes the centre of gravity of the body. The symbols are explained in Table 1.

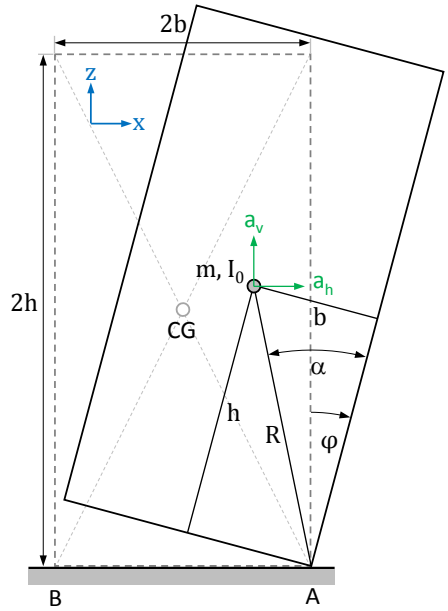

Figure 1: Plane model of a rigid body

Symbol	Parameter
2h	height
2b	width
$R = \sqrt{b^2 + h^2}$	length of the half diagonal
φ	angle of rotation
m	mass
I_0	moment of inertia about CG
$I = I_0 + mR^2$	moment of inertia about A/B
α	critical angle of rotation
$b/h = \tan\alpha$	aspect ratio
g	acceleration of earth gravity
$a_h(t)$	horizontal seismic acceleration
$a_v(t) + g$	vertical seismic acceleration
$p = \sqrt{mgR/I}$	frequency parameter
r	coefficient of restitution
E	modulus of elasticity

Table 1: Important characteristics and parameters

Assuming that the coefficient of friction is large enough, so that there is no sliding, the dynamic equilibrium conditions for the moments about the points A and B give the following equations of motion for the rigid body, which are also known from the literature [1] to [5]:

$$\begin{aligned} &\ddot{\varphi} - p^2 \left\{ \frac{a_v(t)}{g} \sin(\alpha - \varphi) + \frac{a_h(t)}{g} \cos(\alpha - \varphi) \right\} = 0, \ \varphi > 0 \qquad \text{(Point A)} \\ &\ddot{\varphi} + p^2 \left\{ \frac{a_v(t)}{g} \sin(\alpha + \varphi) - \frac{a_h(t)}{g} \cos(\alpha + \varphi) \right\} = 0, \ \varphi < 0 \qquad \text{(Point B)} \end{aligned} \tag{1}$$

Or as a single equation:

$$\ddot{\varphi} - p^2 \left\{ \operatorname{sgn}(\varphi) \frac{a_v(t)}{g} \sin(\alpha - |\varphi|) + \frac{a_h(t)}{g} \cos(\alpha - |\varphi|) \right\} = 0 \tag{2}$$

The term $\operatorname{sgn}(\varphi)$ denotes the signum-function:

$$\operatorname{sgn}(\varphi) = \begin{cases} -1 & \varphi < 0 \\ 0 \quad \text{for} & \varphi = 0 \\ 1 & \varphi > 0 \end{cases}$$

For a homogeneous rectangular block

$$I_0 = \frac{m}{3}(b^2 + h^2) \quad \text{and} \quad p^2 = \frac{3}{4}\frac{g}{R}.$$

When the condition

$$|a_h(t)| \leq |a_v(t)| \tan \alpha \tag{3}$$

is satisfied, rocking motion is not initiated and the body remains at rest. For $\varphi > \alpha$ the body will overturn if there is no restoring moment from the horizontal earthquake acceleration. In the case of pure rocking the Equations (1) or (2) give the motion before and after the impact. These equations are coupled by the angular velocities immediately before and after the impact. Housner [1] has derived a model to calculate the angular velocity of the rigid body after the impact and the energy dissipation during the impact. The model uses the following assumptions:

- The body and the base are rigid.
- There is no bouncing or complete lifting off of the body.
- The impact is a point impact (point contact).
- The time interval of the impact is very short.
- The body remains at the same position during the impact time.

Under these assumptions the principle of conservation of angular momentum immediately before and after the impact gives the following equation for the rigid body:

$$I\dot{\varphi}_{(+)} = I\dot{\varphi}_{(-)} - 2mbR\dot{\varphi}_{(-)} \sin \alpha \tag{4}$$

($\dot{\varphi}_{(-)}$ - angular velocity before the impact, $\dot{\varphi}_{(+)}$ - angular velocity after the impact)

From this follows the simple relation:

$$\frac{\dot{\varphi}_{(+)}}{\dot{\varphi}_{(-)}} = r = 1 - \frac{2mR^2}{I}\sin^2\alpha \quad \text{or for a rectangular block} \quad \frac{\dot{\varphi}_{(+)}}{\dot{\varphi}_{(-)}} = 1 - \frac{3}{2}\sin^2\alpha \qquad (5)$$

The value r denotes the coefficient of restitution in literature. Combining the Equations (1) or (2) and Equation (5) it is possible to solve the problem piecewise numerically. For the ratio of the kinetic energy before W_k^- and after the impact W_k^+ follows using (5):

$$\frac{W_k^+}{W_k^-} = \frac{\frac{1}{2}I\dot{\varphi}_{(+)}^2}{\frac{1}{2}I\dot{\varphi}_{(-)}^2} = r^2 = \left[1 - \frac{2mR^2}{I}\sin^2\alpha\right]^2 \qquad (6)$$

Since $r < 1$ the impacts have to be inelastic. During the impact kinetic energy is dissipated mainly by energy radiation into the foundation. Other possible mechanisms for dissipation are plasticity and friction. Equation (5) gives the maximum value for the coefficient of restitution for which a rigid body will undergo rocking motion. For $\alpha = \arcsin\sqrt{2/3} \approx 54.74°$ and therefore $b/h = \sqrt{2}$ the body stays in rest after the first impact. It is noted that the value of r according to the Equation (5) and consequently the energy dissipation according to (6) depends only on the geometry and mass distribution of the body. Since this also applies to the equations of motion the rocking of a rigid body (on a rigid base) is completely determined by the geometry and the accelerations. For a (homogeneous) rectangular block the height h and the width b are the important geometrical parameters.

For the case of a free rocking motion after an initial angular displacement φ_0 of the rigid body follows from (1):

$$\ddot{\varphi} \pm p^2 \sin(\alpha \mp \varphi) = 0 \qquad \text{(signs like in Equations (1))} \qquad (7)$$

For the angular velocity after the nth impact a simple consideration of the potential and kinetic energy gives the following equation:

$$\dot{\varphi}_n = r\dot{\varphi}_{n-1} \quad \text{with} \quad \dot{\varphi}_0^2 = \frac{2mgR}{I}\{\cos(\alpha - \varphi_0) - \cos\alpha\} \quad \text{and} \quad n = 1, 2, \ldots \qquad (8)$$

The kinetic energy W_k^n after the nth impact has the value:

$$W_k^n = \frac{1}{2}I\dot{\varphi}_0^2\, r^{2n} \qquad (\dot{\varphi}_0 \text{ from the Equation (8)}) \qquad (9)$$

For small angles $(\alpha - \varphi) \ll 1$ (slender bodies) it is possible to linearize the Equations (7) by using the well-known approximations $\sin(\alpha - \varphi) \approx \alpha - \varphi$ and $\cos(\alpha - \varphi) \approx 1$ and to solve the obtained equation analytically:

$$\ddot{\varphi} \mp p^2\varphi = \mp p^2\alpha \qquad \text{with the solution} \qquad \varphi(t) = \alpha \mp (\alpha \mp \varphi_0)\cosh(pt). \qquad (10)$$

The angle φ_0 denotes the initial angular displacement (or initial rotation). This solution can be used to calculate the time period T (the time for the first rocking cycle) as a function of the initial angle φ_0:

$$T = \frac{4}{p}\cosh^{-1}\frac{1}{1-\frac{\varphi_0}{\alpha}} \tag{11}$$

Equation (11) can be used for an estimation of the natural frequencies of a rocking body.

The Equations (1) or (2) determine together with Equation (5) under the stated assumptions completely the rocking motion of a rigid body. For a rocking motion to take place after the impact, a significant part of the kinetic energy of the body (minimum of 51 % for a rectangular block with $h/b = 2$) has to be dissipated into the foundation during the impact. In other cases the body will perform complicated kinds of motion like bouncing or jumping. Further attempts to understand the impact and the motion after the impact are given in [9], [10], [16] and [21]. The Equations (1) or (2) were derived under the assumption that rocking and sliding motions do not occur at the same time. The equations of motion for a simultaneous occurrence of rocking and sliding motion are given in [2], [10], [19] and [22].

3 NUMERICAL ANALYSES

3.1 Analysis methods

The numerical solution of the Equations (1) or (7) is done by using the (explicit) classical fourth-order Runge-Kutta method with a maximum time step of 0.001 s and an additional method for the accurate determination of the contact time. For every new time step the contact condition $\varphi_n \cdot \varphi_{n+1} \leq 0$ (φ_n - rotation of the current step, φ_{n+1} - rotation of the new step) is checked. In the case of contact, the time interval will decrease until the specified accuracy of the angle φ is reached. Because the Runge-Kutta method also provides the velocity for every time step, the velocity immediately before the impact $\dot{\varphi}_{(-)}$ is given. The procedure is restarted with the initial conditions for the angular displacement $\varphi(t_c) = 0$ and the angular velocity $\dot{\varphi}_{(+)}$ immediately after the impact according to Equation (5), where the time t_c denotes the contact time. For solving Equations (7) the velocity after the impact can be calculated by Equation (8) as well. A comparison of the numerically and analytically determined velocities shows an excellent agreement. For the case of no initial displacement, Equation (3) is used to test if the rocking motion can be initiated. The numerical solutions of Equations (1) or (7) will be mostly used as a reference (quoted as theoretical curve) for the further finite element analyses.

In most publications the authors developed (analytical) mechanical models to describe the motion of the rigid body and used numerical methods for the solution. There are only few works [23] to [26] on this issue using finite element (FE) analyses. FE analyses allow the consideration of elastic or plastic properties of the material, especially of the base. Additionally, the influence of geometrical parameters and their variations from the ideal geometry can be studied. By using infinite elements for the base it is also possible to take the radiation of energy in the foundation into account. Of particular interest is the influence of these parameters on the coefficient of restitution, which can be simply calculated from the ratio of the kinetic energies of two successive maxima. The FE analyses use the implicit code of the program Abaqus [27]. It is also of interest to determine if an implicit finite element program can be used to solve such problems. Because the impacts have the main influence on the further movement in most analyses, the excitation was done by an initial angular displacement $\varphi_0 < \alpha$. After preliminary calculations a maximum time increment of 0.001 s and automatic time stepping will be used for all calculations from now on.

3.2 Analyses for initial displacements

The first FE analyses were done with the discrete and abstract FE model in Figure 2 using rigid R2D2 elements for the geometry of the body and SPRING1 (a spring between a node and ground) or DASHPOT1 (a dashpot between a node and ground) elements for the base. The value c denotes the spring stiffness and k the damping constant. With a high stiffness and no damping this FE model is very similar to the analytical model. The results for a rectangular block with an aspect ratio of 2 and a nearly rigid base with stiffness $c = 2 \cdot 10^{16}$ N/m and without damping are shown in Figure 3 and 4. In addition, the curves resulting from Equation (7) for the best estimate coefficient of restitution $r = 0.69$ are given in the figures. The time history of the kinetic energy normalized to the maximum in Figure 3 shows as a result of the FE analyses that the block is bouncing and jumping multiple times during the impact. However, the theoretical curve from Equation (7) can be considered as a global approximation of the time history obtained by the FE analysis. In spite of the multiple bouncing and jumping during the impacts, the differences between the theoretical and the FE curves for the relative angular displacements φ/α are relatively small.

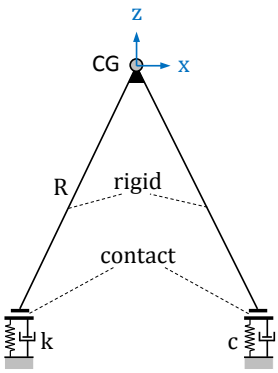

Figure 2: Rigid FE model with spring and damper

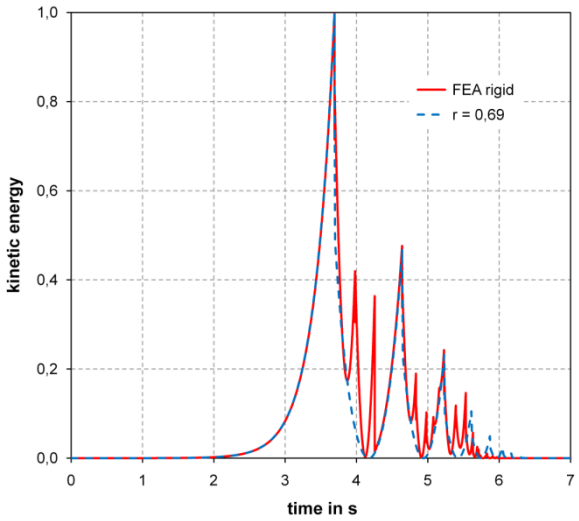

Figure 3: Time histories of the kinetic energy for the model with a rigid body on a nearly rigid base

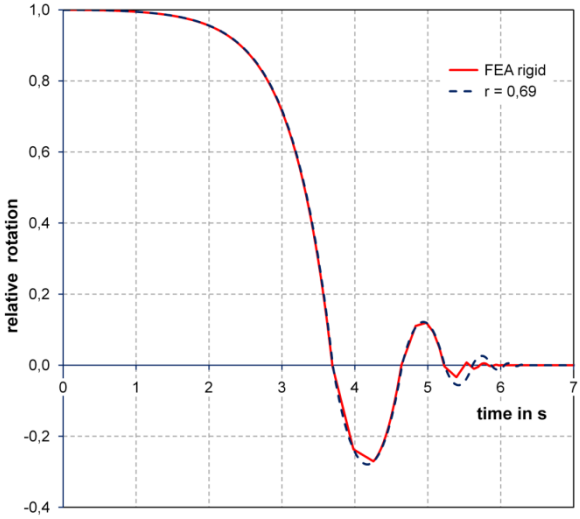

Figure 4: Time histories of the relative rotation for the model with a rigid body on a nearly rigid base

A basic problem of the previously used rigid model is that the rigid base does not dissipate energy during the impact. Therefore, additional analyses were done with the same model but using a smaller stiffness $c = 2 \cdot 10^{10}$ N/m and a damping value $k = 1{,}4 \cdot 10^{8}$ kg/s. The dimensions of the rectangular block are 2 m x 2 m x 4 m (width/depth/height), the mass is 124.8 t (similarly to a storage cask). The results obtained for a rigid block with an h/b-ratio of 2 are presented in the Figures 5 and 6. There is no bouncing or jumping with these values for the parameters c and k. Other combinations of c (especially large c) and k often produce bouncing and/or jumping. The comparison between the curves of the FE analysis and those from Equation (7) show a very good agreement. The curves resulting from Equation (7) for the best estimate coefficient of restitution $r = 0.7$ are also given in the figures. The coefficient of restitution of 0.7 is identical with the value from Equation (5) but decreases slightly from 0.7 to 0.69. A problem is the determination of the real stiffness and damping of the ground.

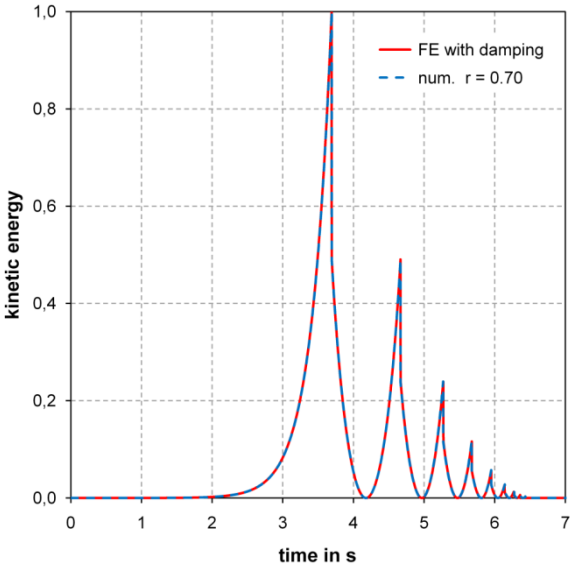

Figure 5: Time histories of the kinetic energy for the FE model with spring and damper

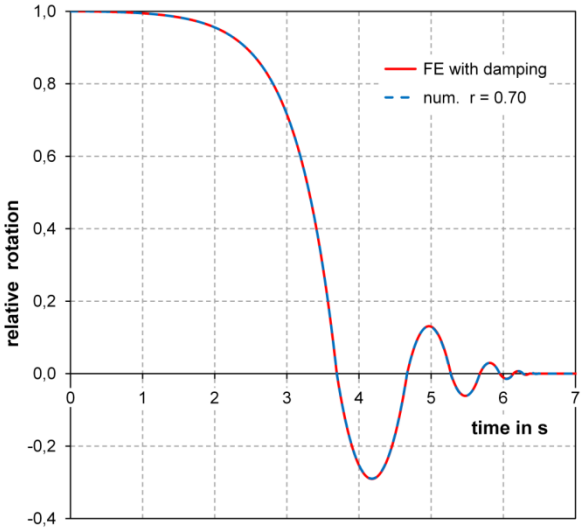

Figure 6: Time histories of the relative rotation for the FE model with spring and damper

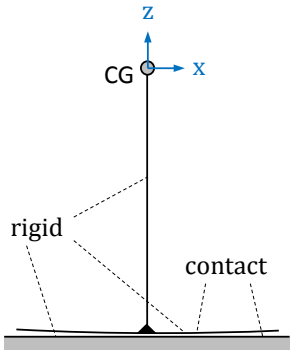

Figure 7: Rigid model with a curved contact line

In the analytical but also in the FE model in Figure 2 the rotation point changes immediately (or in a very short time) and discontinuously from one corner point to the other. To simulate a continuous transition of the rotation centre from corner to corner, the model in Figure 7 with a curved contact line is investigated. The curvature may be considered as a very small deviation from the ideal straight line geometry. Figures 8 and 9 show the time histories of the normalized kinetic energy and the relative angular displacement for a block with an aspect ratio of 2 for three different radii. With the radii used, the deviations between the two bottom corner points of the block and the ideal geometry of the rectangular block are only 0.1 mm, 0.5 mm und 1.0 mm, respectively.

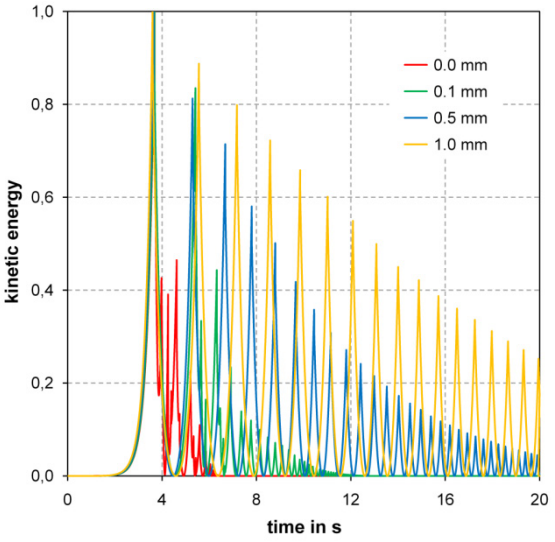

Figure 8: Time histories of the kinetic energy for the model with a curved bottom and b/h = 2

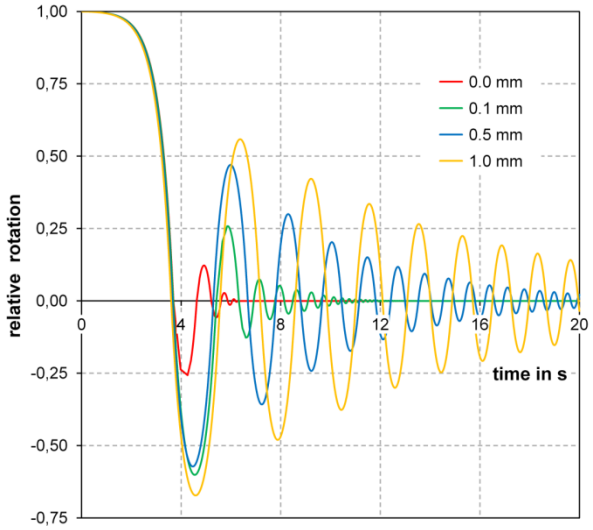

Figure 9: Time histories of the relative rotation for the model with a curved bottom and b/h = 2

Despite the very small deviation from the ideal geometry (in respect to the width of the block of 2 m only 0.05 ‰ to 0.5 ‰), the differences between the curves are very large. In all cases with the exception of the reference (0.0 mm) the coefficients of restitution are significantly greater than the value from Equation (5) and reach a maximum value of about 0.95. It is remarkable, that for a deviation of only 0.1 mm the coefficient for the first impact is already 0.9. Although the considered deviations are idealized, the obtained results show that very small geometrical deviations produce significantly larger coefficients of restitution and therefore different curves.

The previous models are not classical FE models because they use rigid bodies and have no real stiffness. Therefore, in the next step, the plane FE model in Figure 10 with CPS4 and CINPS4 elements (plane stress elements) is considered. The block is rigid by using the 'rigid body'-constraints in the FE model. In the regions of the contact points the mesh is refined. For the base one row of the infinite elements CINSP4 is used. These elements do not reflect elastic waves on the boundaries of the model. Without the thereby resulting radiation of energy into the foundation, the impact will excite elastic base vibrations, which especially without additional damping influence the impact. For comparison with the other models the first calculations were performed with a relative stiff base (modulus of elasticity E = 1000 GPa, density 7800 kg/m³). Figures 11 and 12 show the results obtained for a block with h/b = 2 and a mass of 124.8 t (similar to a typical storage cask). During the first impact a slight bouncing and jumping occurs. There is a very good agreement between the theoretical (numerical integration of Equations (1)) and the FE results, if a coefficient of restitution of 0.75 is used instead of the theoretical value 0.7 according to Equation (5).

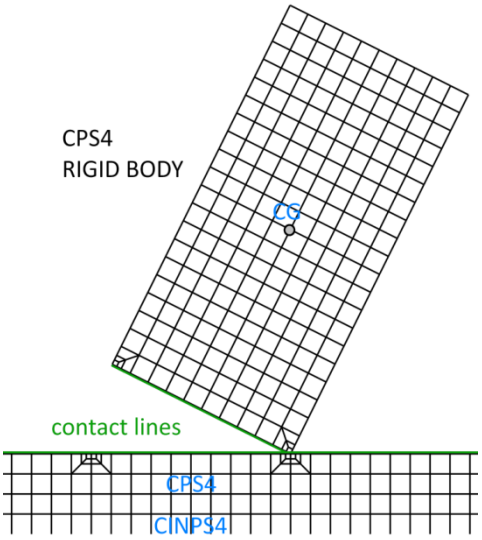

Figure 10: Plane FE model using a rigid body, CPS4 and CINSP4 elements

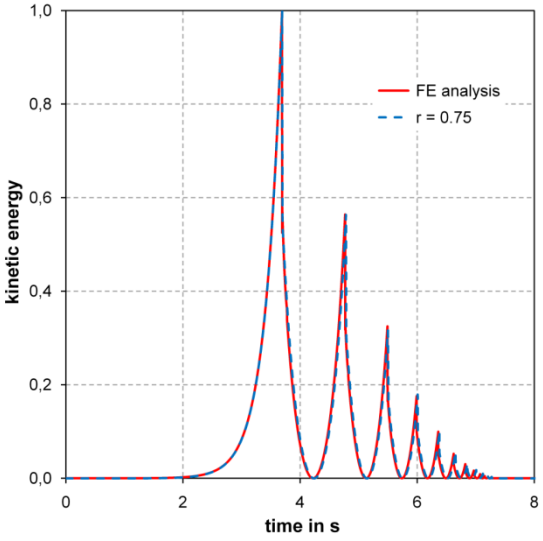

Figure 11: Time histories of the kinetic energy for the plane FE model with a very stiff base

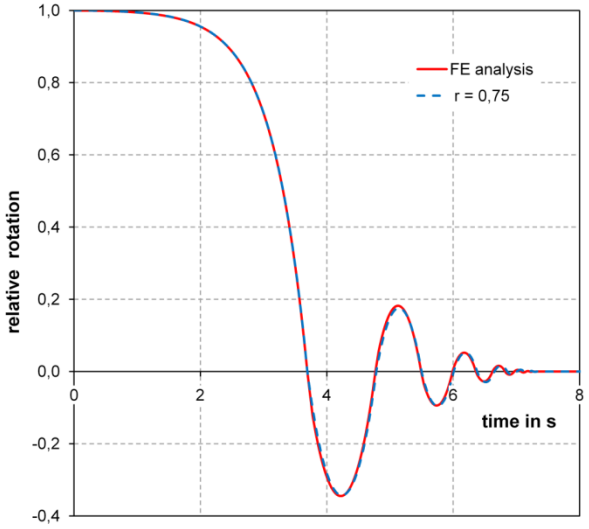

Figure 12: Time histories of the relative rotation for the plane FE model with a very stiff base

The previously used model has been modified with respect to the contact conditions and a smaller stiffness of the base (E = 200 GPa). In the case of point contact the contact occurs on the two corners. The case of the line contact is shown in Figure 10. In the last case the corners (edges) are slightly bevelled (0.5 mm on a length of 25 mm). The results are presented in Figures 13 und 14. As expected, the contact conditions have a significant influence on the coefficient of restitution and the time histories. The coefficients have the maximum values 0.72, 0.76 und 0.82 for the three respective contact conditions. The theoretical value is 0.7.

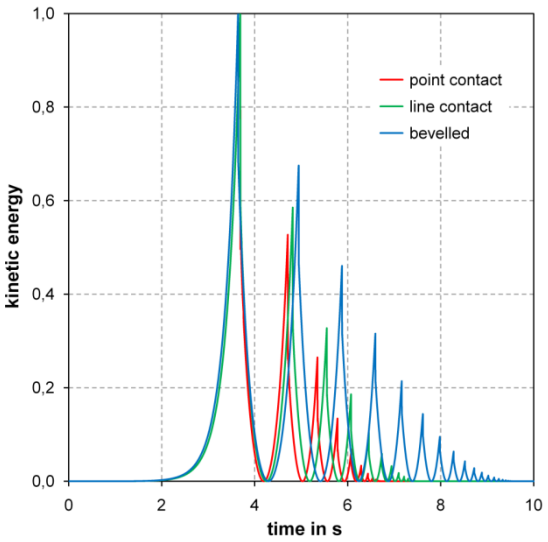

Figure 13: Time histories of the kinetic energy for the plane model with different contact conditions

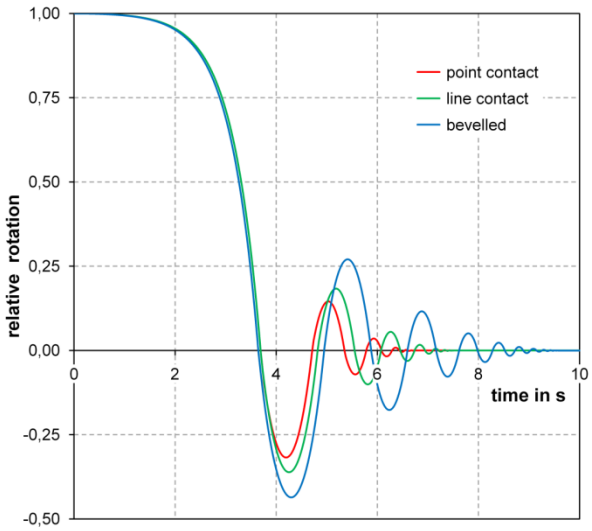

Figure 14: Time histories of the relative rotation for the plane model with different contact conditions

To study the influence of the plasticity, additional calculations were done using an ideal elastic-plastic material for the base. The materials have a modulus of elasticity of 200 GPa and a yield stress of 200 MPa (similar to austenitic steel, block mass 124.8 t), as well as a modulus of 35 GPa and a yield stress of 50 MPa (similar to concrete, mass 35.2 t). The results and the theoretical curves for the best estimate coefficients r are shown in Figures 15 and 16.

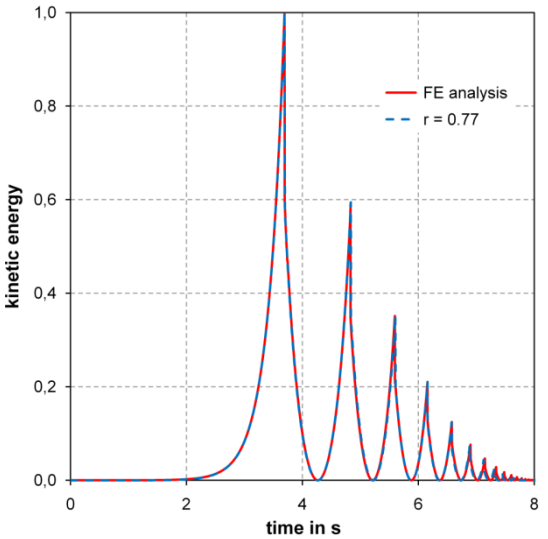

Figure 15: Time histories of the kinetic energy for a model with an elastic-plastic material like steel

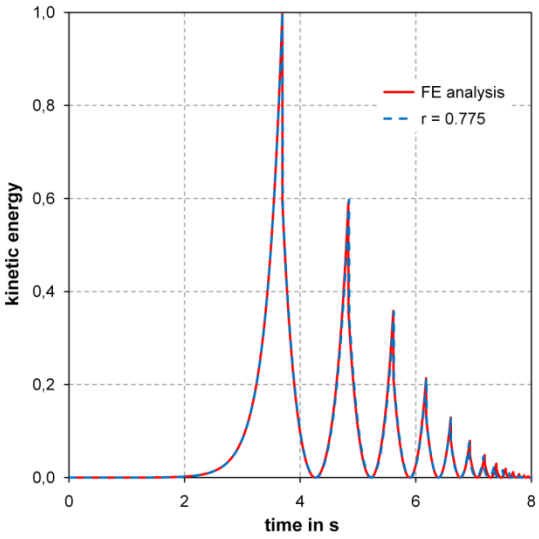

Figure 16: Time histories of the kinetic energy for a model with an elastic-plastic material like concrete

There is a very good agreement between the theoretical and the FE results in both figures if the coefficients of restitution stated in the figures are used instead of the theoretical value 0.7. The differences between the two best estimate coefficients in the figures 0.77 and 0.775 are very small, but again significantly larger than the theoretical value. In the range below 10 % of the maximum kinetic energy and therefore for small amplitudes, the agreement between the two curves becomes lower, which may indicate a dependence of the coefficient on the amplitude. Because of the small values of the kinetic energy this question cannot be resolved completely.

In many cases anti-slip pads are used to prevent sliding. To investigate the effect of such a pad on the motion, the model is modified by a 1 cm thick mat between the body and the base. The material of the pad is assumed to be elastic with a modulus of 50 MPa (density 1200 kg/m³, Poisson ratio 0.49). There is no bouncing and jumping, but because of the low horizontal stiffness a horizontal oscillation of the rotation point occurs at large deflections in addition to the rocking motion. The results are shown in Figures 17 and 18. The coefficient of restitution reaches values around 0.9 and varies in some cases from impact to impact. The initial impact is done after 3.05 s, in difference to the approximate 3.69 s for all other models. The curves in Figure 17 und 18 can no longer be described using Equation (1) or (2).

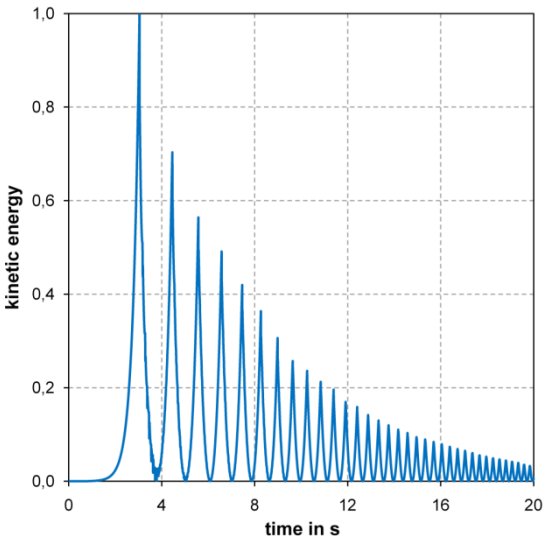

Figure 17: Time history of the kinetic energy for a rigid block with an anti-slip pad

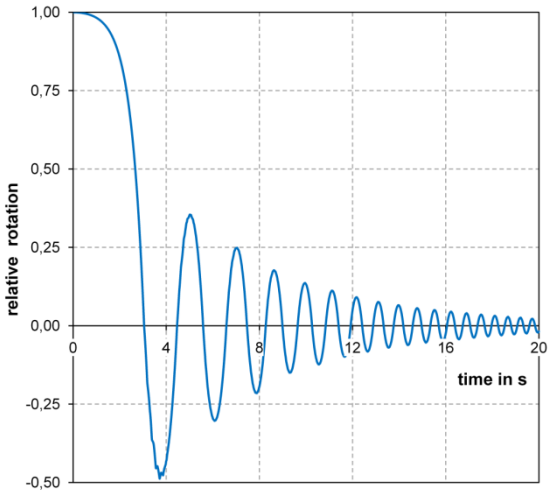

Figure 18: Time history of the relative rotation for a rigid block with an anti-slip pad

Additional FE analyses with 3D models give similar results and dependencies, so there is no reason for an additional presentation of these results. These models will be used for future studies under multiaxial excitation.

3.3 Analyses with dynamic excitations

The dynamic response of the body does not only depend on the geometric parameters and the coefficient of restitution but also on the type and strength of the excitation. Therefore, the excitation is further investigated. Because the previous studies have shown a very good agreement between the numerical solutions of Equation (1) with the best estimate coefficient of restitution (calculated by FE analyses) and FE analyses, most calculations are performed by using the numerical integration of the equations of motion.

In the first case, the block is excited by sine, triangle or rectangle vibrations with an ampli-

tude of 1 g (about 9.81 m/s²) and a frequency of 1 Hz. The results obtained for the block with h/b = 2 using a coefficient of restitution of 0.7 and 0.85 are shown in Figures 19 and 20. As expected, the largest displacements are caused by rectangle vibrations. The maximum rotation is usually found during the first four impacts. It is remarkable, that in the case of an excitation with rectangle vibrations and using the conservative coefficient of restitution of 0.8, the amplitudes will increase significantly over time until overturning. For a verification of the results, some FE analyses with the model in Figure 10 with h/b = 2 (mass 124.6 t) on an elastic base (E = 200 GPa, density 7800 kg/m³) have been performed. The curves in Figure 21 confirm the previous statements about the very good agreement between theoretical and FE results. Figure 22 illustrates the dependency of the maximum rotation at an excitation using sine or rectangle vibrations. For a assumed sine oscillation of the block the dependency of the maximum amplitude φ_{max} on the frequency f is given by the relation $\varphi_{max} \sim 1/f^2$. The dependency in Figure 22 corresponds to a power slightly over 2.

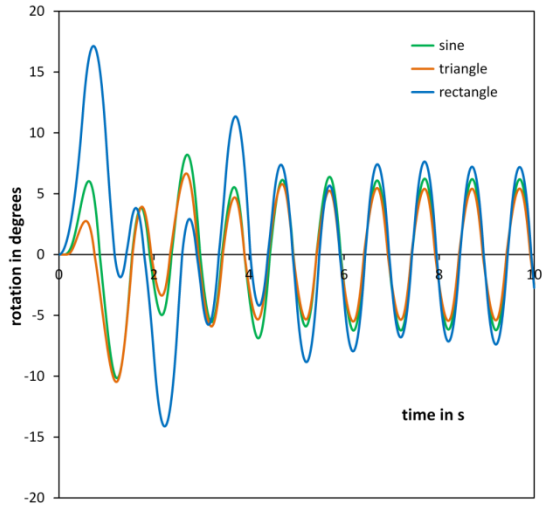

Figure 19: Time history of the rotations for different excitations with r = 0.7 and a frequency of 1 Hz

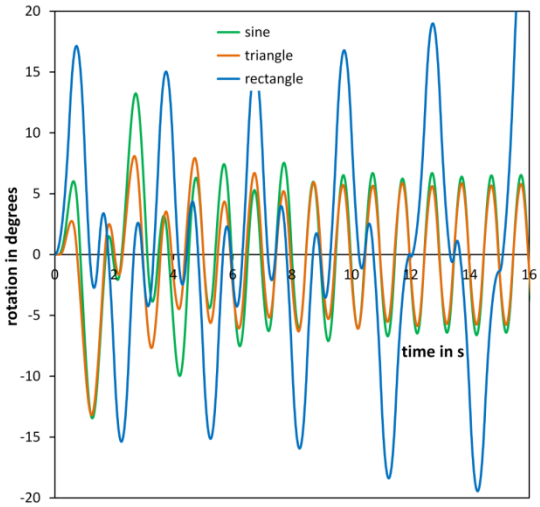

Figure 20: Time history of the rotations for different excitations with r = 0.85 and a frequency of 1 Hz

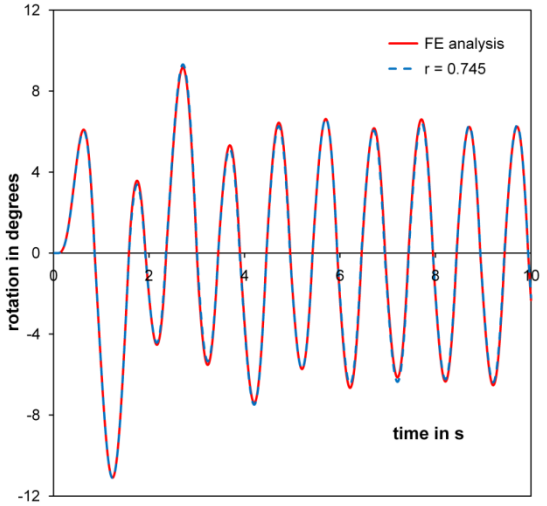

Figure 21: Time history of the rotations for an excitation with a sine vibration 1 Hz

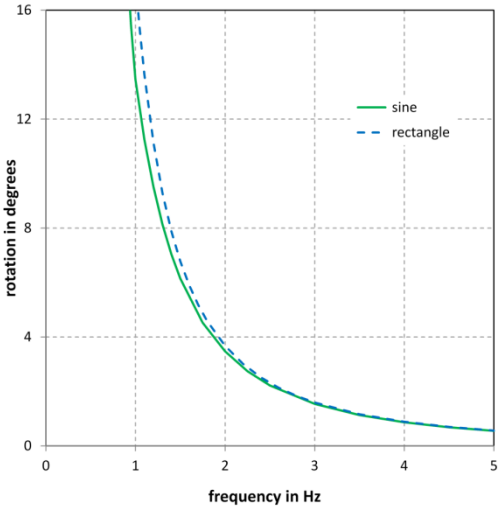

Figure 22: Maximum angular displacements for different excitations with r = 0.85

Additionally, calculations are done with time histories using earthquake ground accelera-

tions from the European strong-motion database. As examples two time histories of earthquake ground accelerations are shown in Figures 23 and 25. Both time histories are normalized to peak ground accelerations (PGA) at 1 g. The calculations use the previously described method for the numerical integration of the equations of motion. The resulting motions of a rigid block with h/b = 2 using the conservative coefficient of restitution of 0.8 are presented in Figure 24 and 26. The maximum rotations are about 0.5° and 1.7°. Further calculations for other additional time histories cause an even greater variation in the results.

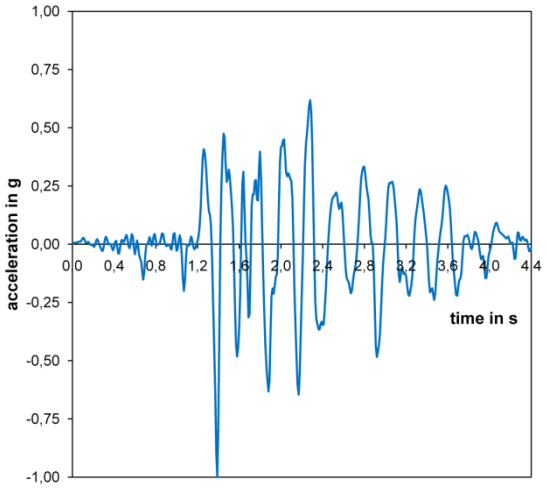

Figure 23: Time history of the acceleration for the Albstadt earthquake (Germany, 16.01.1978)

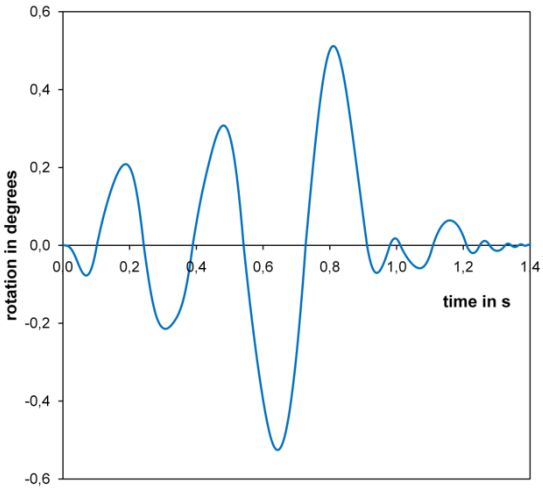

Figure 24: : Time history of the rotations for the Albstadt earthquake with r = 0.8

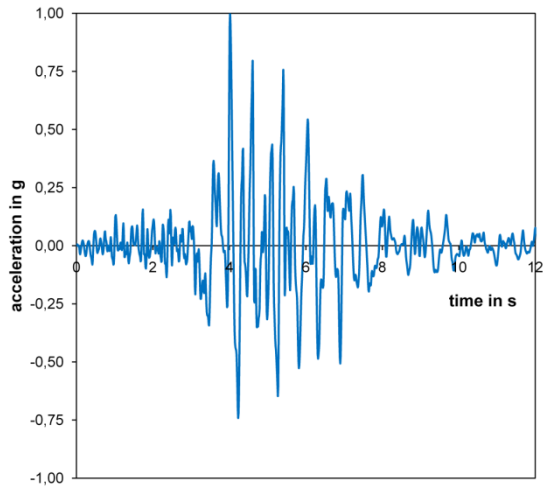

Figure 25: Time history of the acceleration for the Friuli earthquake (Italia, 06.05.1976)

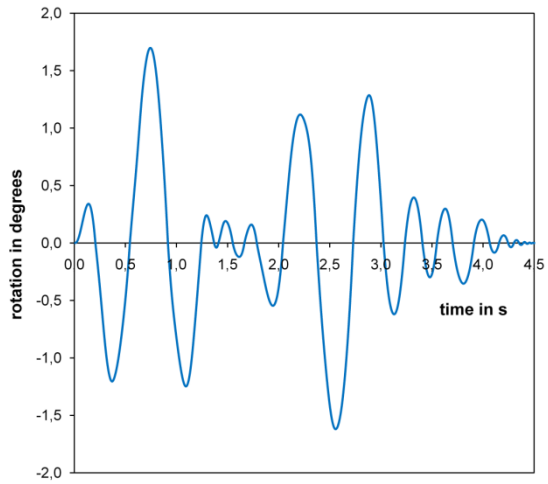

Figure 26: : Time history of the rotations for the Friuli earthquake with r = 0.8

Because the previous studies investigate only pure rocking motions, now the transition between rocking and sliding motion will be shortly considered. For the FE analyses the model in Figure 10 (h/b = 2, mass 124.6 t, E = 200 GPa, density 7800 kg/m³) is used. The results for coefficients of friction μ between 0.1 und 1.0 show that for μ = 0.6 the block performs a (nearly) pure rocking motion. For μ = 0.55 it is a combined rocking and sliding motion with an amplitude of about 68 mm. For μ = 0.5 the amplitude of sliding amounts to about 300 mm. For μ = 0.45 the block performs a pure sliding motion with an amplitude of about 390 mm. The motion is very sensitive to small changes of the geometry of the base.

4 CONVENTIONAL AND NUCLEAR RULES

The European standards EN 1990 [33] and EN 1998 [34] and the US standard ASCE 7-10 [30] give design criteria for rocking and sliding of structures in non-nuclear facilities. For nuclear facilities the US standard ASCE/SEI 43-05 [29] and the German KTA 2201.1 [35] and KTA 2201.4 [36] provide guidance for analysis of rocking and sliding.

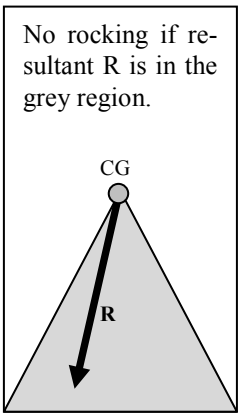

Figure 27: Static evaluation of rocking stability

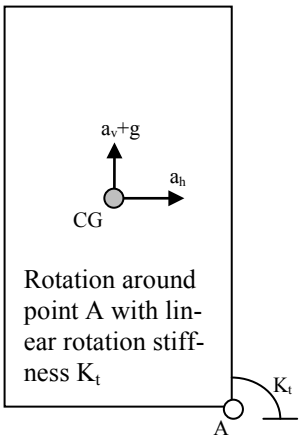

Figure 28: Model of ASCE/SEI 43-05, Appendix A.2 for the determination of the rocking angle φ_{max}

The easiest way to show that a body will not tip over is to show that the resultant force due to gravity and the seismic accelerations is within the grey area of Figure 27. This criterion prevents rocking. It is used by all the standards mentioned above except the standard ASCE/SEI 43-05. In order to see how large the safety factors are, Table 2 shows how the dead load component is determined for the different standards. The value of the vertical seismic acceleration is also given.

Code	ASCE/SEI 7-10	EN 1990 and EN 1998	KTA 2201.1 and 2201.4
Factor for dead load	0.9	1.0	0.95
Upward seismic load	Two-thirds of the horizontal seismic acceleration	30 % of the vertical seismic acceleration (permitted to be neglected if the vertical PGA is less than 0.25 g)	30 % of the vertical seismic acceleration, which can be assumed to be two-thirds of the horizontal seismic acceleration

Table 2: Static evaluation of rocking stability of a rigid body

Standard ASCE/SEI 43-05 gives an approximate method for the determination of the best estimate rocking angle φ_{max} for given spectral accelerations. How these formulas were derived is mentioned in Appendix B.2 of the standard. The main idea is to reduce the nonlinear system to a linear system, where the body rotates around its corner and is restraint by a linear torsion spring (see Figure 28). The spring's torsion coefficient K_t is determined in such a way that at the maximum rocking angle φ_{max} the energy of the spring equals the potential energy of the φ_{max} inclined body. With these assumptions, the governing equation is that of the well-known single degree of freedom system:

$$I\ddot{\varphi} + 2D\sqrt{K_t I}\dot{\varphi} + K\varphi = m\{a_h h + (a_v + g)b\} \tag{12}$$

$$\text{with} \qquad K_t = \frac{2mgh}{\varphi_{max}^2}\left\{\cos\varphi_{max} + \frac{b}{h}\sin\varphi_{max} - 1\right\} \tag{13}$$

As defined in Table 1, $(a_v + g)$ denotes the vertical seismic acceleration. With this model it is possible to use given design spectra of an earthquake for the determination of φ_{max}. The rotation due to the vertical and horizontal earthquake acceleration is combined by the square root of the sum of the squares (SRSS). The damping factor of the spectrum is based on the coefficient of restitution. The equivalent viscous damping is derived in such a way, that the energy loss per cycle of the free oscillating linear system of Figure 28 equals that of the system in Figure 1 and Equation (5). For a homogeneous rectangular block with h/b = 2 the damping factor D is 11.3 %. The rotations are best estimate values and the maximum rocking angle has to be multiplied by a safety factor of 2.0. Because the real system is simplified by this method, the question arises, if this method is sufficiently proven for all types of bodies.

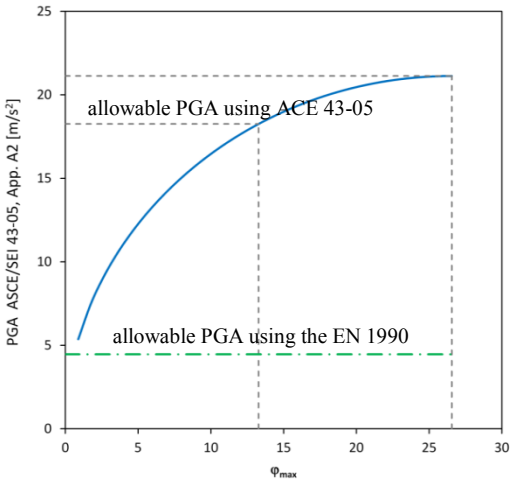

Parameters
Rigid body
2h = 4 m
2b = 2 m
Instability angle α = 26.6 °
Elastic Spectrum type 1 acc. to EN 1998
Ground type A = Rock
Vertical seismic acceleration equals 2/3 horizontal acceleration

Figure 29: Allowable peak ground acceleration and effect of the safety factor = 2.0 of ASCE 43-05

Figure 29 shows the allowable peak ground acceleration (PGA) according to ASCE/SEI 43-05 using a spectrum which is given in EN 1998. For the given geometry the safety factor of 2.0 applied to the deformation results in a much smaller safety factor regarding the allowable PGA. The allowable PGA according to the ASCE/SEI 43-05 is 4.1 times higher than that derived from a static evaluation according to Table 2 using the Eurocode procedure.

Comparison of ASCE 43-05 Appendix A Results with NUREG/CR-6865 Time History Results

μ = 0.80, RG 1.60, All Soil Profiles
Critical Angle = 29.2 degrees

	Median Peak Cask Rotation (Degrees)	
PGA	NUREG/CR-6865 Median	ASCE 43-05 App. A, 10% Damping
0.25	0.1	0
0.40	1.2	0.8
0.50	3.7	1.4
0.60	9.1	2.1
0.80	37.9	4.4
1.00	114.0	7.9

Table 3: Comparison of ASCE 43-05 with time history analyses (μ - coefficient of friction, from [23])

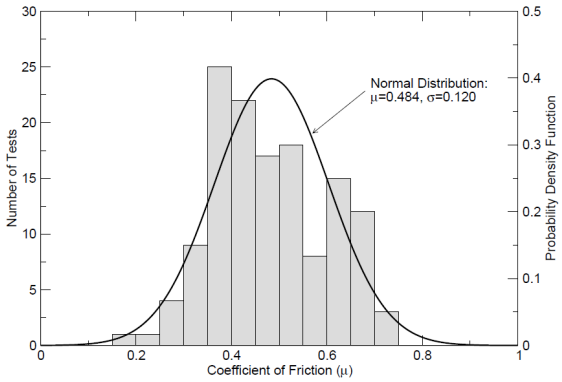

Figure 30: Histogram of steel/concrete coefficient of friction test results (published in [23])

The U.S. Nuclear Regulatory Commission (NRC) published a presentation [23] where Table 3 is shown. It summarizes the results of different time history analyses using the FE code Abaqus explicit and compares it to ASCE/SEI 43-05 results. The rocking body is a cylindrical cask. ASCE/SEI 43-05 predicts much smaller angles φ_{max}. A cylindrical body may roll around its edge, which leads to less energy dissipation.

According to [37] a new revision of the standard ASCE 4-98 is planned to provide guidance for analysis of rocking and sliding of unanchored bodies subjected to seismic load based on ASCE/SEI 43-05. Up to now it has not been published.

All mentioned codes above except ASCE/SEI 43-05 prevent sliding by checking that the horizontal force divided by the resultant vertical force is less than the existing friction coefficient. The ASCE/SEI 43-05 in Appendix A.1 provides a procedure for computing a best estimate sliding distance. This procedure needs the spectrum and the coefficient of sliding at the 95 % exceedance level as input data. The procedure is stated as conservative and the result shall be increased by a safety factor of 2.0. The safety factor 3.0 is necessary for best estimate sliding distances derived from time history analyses (mean value of at least five time histories). Figure 30 shows test results of the steel/concrete coefficient of friction.

5 SUMMARY

The rocking motion of unanchored bodies under seismic excitation was investigated by numerical integration of the equations of motion and with the Finite Element Method. For numerical integration the classical fourth-order Runge-Kutta method and for the finite element analyses the programs Abaqus (implicit code) were used.

An important part of the investigations is the calculation of the coefficient of restitution with FE analyses. The results obtained from calculations for a rectangular block with an aspect ratio of 2 for models with geometric variations, different contact conditions and different properties of the base result in the following conclusions for the case of an initial angular displacement:

- Rigid FE models without additional damping are not suitable because they produce an unrealistic bouncing and jumping. For 2D or 3D FE models the usage of infinite elements is recommended.

- In most cases the agreement between results from FE analyses and the numerical integration of the equations of motion is very good, if the coefficients of restitution are based on best estimate values from FE analyses.

- All variations from the ideal geometry and contact conditions cause larger coefficients of restitution in comparison to the theoretical value 0.7 of the Housner model. The consideration of plasticity gives higher values as in the elastic case. The maximum values for the coefficients are about 0.9. It is recommended to use a value of at least 0.8 for theoretical calculations.

- Some investigations show a dependence of the coefficients of restitution on the amplitude.

- Anti-slip mats lead to greater coefficients of restitution and shorter rocking periods. The usage can only be recommended if the body is compact and overturning not a problem.

The dynamic investigations consider an excitation by sine, triangle or rectangle vibrations and time histories from earthquake ground accelerations. The calculations for a rectangular block with an aspect ratio of 2 result in the following conclusions:

- The agreement between results from FE analyses and the numerical integration of the equations of motion is very good if the coefficients of restitution are based on the FE analyses.

- Because of the possible dependence of the coefficients of restitution on the amplitude additional calculations with 2D or 3D FE models are recommended. In the case of a horizontal and vertical excitation 2D models provide a good accuracy.

- Calculations for coefficients of friction between 0.1 und 1.0 show, that for values below 0.45 the block performs a pure sliding motion. For 0.5 to 0.55 it is a combined rocking and sliding motion. The motion is very sensitive to small changes of the geometry of the base or the body.

- Because of the large variations of the results the investigation of a large number of time histories is recommended.

Additionally, it will be noted that implicit FE programs are suitable to study the rocking and sliding problem.

All investigated codes prevent rocking by the requirement that the overturning moment at the base is less than the resisting moment due to dead load minus the vertical seismic acceleration. Sliding is prevented by checking that the required coefficient of friction is smaller than the existing one. From the mechanical point of view the mentioned rocking proof of the codes is correct and needs no assumptions. It is a lower bond value. The standard ASCE/SEI 43-05 provides a procedure for the determination of a best estimate rocking angle due to seismic accelerations beyond the lower bond value. By linearizing the highly nonlinear phenomenon it is possible to use design spectra. There are no restrictions with regard to the type of body. The question if the procedure of ASCE/SEI 43-05 is sufficiently conservative for all geometries of rigid bodies cannot be answered. Based on our own investigations and those of the U.S. Nuclear Regulatory Commission there are doubts.

REFERENCES

[1] G.W. Housner, The behavior of inverted pendulum structures during earthquakes. *Bulletin of the Seismological Society of America*, **53**, 403-417, 1963.

[2] Y. Ishiyama, Motions of rigid bodies and criteria for overturning by earthquake excitations. *Earthquake Engineering & Structural Dynamics*, **10**, 635-650, 1982.

[3] M. Aslam, W.G. Godden, D.T. Scalise, Rocking and overturning response of rigid bodies to earthquake motions. LBL-7539, Lawrence Berkeley Laboratory, November 1978.

[4] C.S. Yim, A.K. Chopra and J. Penzien, Rocking response of rigid blocks to earthquakes. *Earthquake Engineering & Structural Dynamics*, **8**, 565-587, 1980.

[5] A.S. Koh, P.-T.D. Spanos, Seismically induced rocking of rigid structures. *Proceedings of Eighth World Conference on Earthquake Engineering*, San Francisco, CA, Vol. IV, 251-258, 1984.

[6] W.K. Tso, C.M. Wong, Steady state rocking response of rigid blocks part 1: Analysis. *Earthquake Engineering & Structural Dynamics*, **18**, 89-106, 1989.

[7] C.M. Wong, W.K. Tso, Steady state rocking response of rigid blocks part 2: Experiment. *Earthquake Engineering & Structural Dynamics*, **18**, 107-120, 1989.

[8] S.J. Hogan, On the dynamics of a rigid block, tethered at one corner, under harmonic forcing. *Proceedings of the Royal Society, Series A*, **439**, 35-45, 1992.

[9] H.W. Shenton III, N.P. Jones, Effect of friction and restitution on rocking response. *Earthquake Engineering, Tenth World Conference*, Balkema, Rotterdam, 1933-1938, 1992.

[10] P.R. Lipscombe, S. Pellegrino, Free rocking of prismatic blocks. *Journal of Engineering Mechanics*, **119**, 1387-1410, 1993.

[11] N. Makris, Y. Roussos, Rocking response and overturning of equipment under horizontal pulse-type motions. *Report PEER-1998/05*, Pacific Earthquake Engineering Research Center, College of Engineering, University of California, Berkeley, 1998.

[12] N. Makris, J. Zhang, Rocking response and overturning of anchored equipment under seismic excitations. *PEER Report 1999/06*, Pacific Earthquake Engineering Research Center, University of California, Berkeley, 1999.

[13] Andreaus, On the rocking-uplifting motion of a rigid block in free and forced motion: influence of sliding and bouncing. *Acta Mechanica*, **138**, 219-241, 1999.

[14] F. Prieto, P.B. Lourenand C.S. Oliveira, Impulsive Dirac-delta forces in the rocking motion. *Earthquake Engineering & Structural Dynamics*, **33**, 839–857, 2004.

[15] M. Apostolou, G. Gazetas, E. Garini, Seismic response of slender rigid structures with foundation uplifting. *Soil Dynamics and Earthquake Engineering*, **27**, 642-654, 2007.

[16] C. Yilmaz, M. Gharib and Y. Hurmuzlu, Solving frictionless rocking block problem with multiple impacts. *Proceedings of the Royal Society, Series A*, **465**, 3323-3339, 2009.

[17] D. Konstantinidis, N. Makris, Experimental and analytical studies on the response of freestanding laboratory equipment to earthquake shaking. *PEER Report 2005/07*, Pacific Earthquake Engineering Research Center, University of California, Berkeley, 2005.

[18] F. Pena, F. Prieto, P.B. Lourenc, A. Campos Costa and J.V. Lemos, On the dynamics of rocking motion of single rigid block structures. *Earthquake Engineering & Structural Dynamics*, **36**, 2383-2399, 2007.

[19] A.N. Kounadis, On the overturning instability of a rectangular rigid block under ground excitation. *The Open Mechanics Journal*, **4**, 43-57, 2010.

[20] H. Zhang, B. Brogliato, Multiple impacts with friction in the rocking block. *Nosmooth contact and impact laws in mechanics (Euromech 2011)*, Grenoble, France, July 6-8, 2011.

[21] H. Zhang, B. Brogliato, The planar rocking-block: analysis of kinematic restitution laws, and a new rigid-body impact model with friction. *Institut National de Recherche en Informatique et en Automatique*, Grenoble - Rhône-Alpes, No. 7580, 2011.

[22] M.-Y. Jeong, I.-Y. Yang, Characterization on the rocking vibration of rigid blocks under horizontal harmonic excitations. *International Journal of Precision Engineering and Manufacturing*, 13, 229-236, 2012.

[23] NUREG/CR-6865. Parametric evaluation of seismic behavior of freestanding spent fuel dry cask storage systems. Sandia National Laboratories, U.S. Nuclear Regulatory Commission, 2005.

[24] Q.T. Ma, J.W. Butterworth and B.J. Davidson, Modelling rocking structures using standard finite elements. *NZSEE Conference*, Wairakei Resort, Taupo, New Zealand, 2005.

[25] S. Lamarche, F. Voldoire, H. Ben Dhia and C. Zammali, Validation of contact-impact approaches for FEM software. *EURODYN 2005*, September 4-7, Paris, France, 2005.

[26] R. Kourkoulis, P. Kokkali, Parametric dimensional analysis on rocking of 1-dof systems. *4th Japan-Greece Workshop on Seismic Design of Foundations and Innovations in Seismic Protection*, September 2-9, Kobe, Japan, 2011.

[27] Abaqus, Version 6.11, SIMULIA (ABAQUS Inc., Providence, USA).

[28] M. Demosthenous, G.C. Manos, Dynamic response of rigid bodies subjected to horizontal base motions. *Earthquake Engineering, Tenth World Conference*, Balkema, Rotterdam, 2817-2821, 1992.

[29] ASCE/SEI 43-05, Seismic design criteria for structures, systems, and components in nuclear facilities. *American Society of Civil Engineers*, Reston, Virginia, USA, 2005.

[30] ASCE/SEI 7-10. Minimum design loads for buildings and other structures. *American Society of Civil Engineers*, Reston, Virginia, USA, 2010.

[31] ANSI/AISC N690-12, Specification for safety-related steel structures for nuclear facilities. *American Institute of Steel Construction*, Chicago, Illinois, USA, 2012.

[32] S.R. Jensen, O. Gurbuz, Sliding and rocking of unanchored components and structures: Chapter 7.6 ASCE 4 Revision 2. *2011 Structures Congress*, Las Vegas, Nevada, April 14-16, 2011.

[33] EN 1990:2002 (A1:2005, A1:2005/AC:2010 D), Eurocode - Basis of structural design, European Standard. *European Committee for Standardization*, Brusseles, Belgium, 2010.

[34] EN 1998-1:2004 (AC:2009 D), Eurocode 8: Design of structures for earthquake re-

sistance - Part 1: General rules, seismic actions and rules for buildings, European Standard. *European Committee for Standardization*, Brusseles, Belgium, 2009.

[35] KTA 2201.1 (2011-11), Design of Nuclear Power Plants against Seismic Events; Part 1: Principles. *German Nuclear Safety Standards Commission (KTA)*, Germany, 2011.

[36] KTA 2201.4 (2012-11), Design of Nuclear Power Plants against Seismic Events; Part 4: Components. *German Nuclear Safety Standards Commission (KTA)*, Germany, 2012.

[37] G. S. Bjorkman, Methodologies Acceptable to the Staff for Performing Seismic Stability Analyses of a Stack-up Configuration within a 10 CFR Part 50 Facility. *U.S. NRC Spent Fuel Storage and Transportation Division*, November 1, 2011.